# Molecular dynamics simulation of chitinase I from Thermomyces lanuginosus SSBP to ensure optimal activity

Faez Iqbal Khan, Krishna Bisetty, Ke-Ren Gu, Suren Singh, Kugen Permaul, Md. Imtaiyaz Hassan & Dong-Qing Wei

Published online: 22 Sep 2016.

Submit your article to this journal 🗗

View related articles 🗗

View Crossmark data 🗗

Taylor & Francis
Taylor & Francis Group

ADVANCES IN MOLECULAR SIMULATION, 2016

# Molecular dynamics simulation of chitinase I from *Thermomyces lanuginosus SSBP* to ensure optimal activity

Faez Iqbal Khan[a] ![ORCID], Krishna Bisetty[b], Ke-Ren Gu[a], Suren Singh[c], Kugen Permaul[c], Md. Imtaiyaz Hassan[d] ![ORCID] and Dong-Qing Wei[a]

[a]School of Chemistry and Chemical Engineering, Henan University of Technology, Henan, China; [b]Department of Chemistry, Durban University of Technology, Durban, South Africa; [c]Department of Biotechnology and Food Technology, Durban University of Technology, Durban, South Africa; [d]Centre for Interdisciplinary Research in Basic Science, Jamia Millia Islamia, New Delhi, India

**ABSTRACT**

The fungal chitinase I obtained from *Thermomyces lanuginosus* SSBP, a thermophilic deuteromycete, has an optimum growth temperature and pH of 323.15 K and 6.5, respectively. This enzyme plays an important task in the defence mechanism of organisms against chitin-containing parasites by hydrolysing β-1, 4-linkages in chitin. It acts as both anti-fungal and biofouling agents, with some being thermostable and suitable for the industrial applications. Three-dimensional model of chitinase I enzyme was predicted and analysed using various bioinformatics tools. The structure of chitinase I exhibited a well-defined TIM barrel topology with an eight-stranded α/β domain. Structural analysis and folding studies at temperatures ranging from 300 to 375 K using 10 ns molecular dynamics simulations clearly showed the stability of the protein was evenly distributed even at higher temperatures, in accordance with the experimental results. We also carried out a number of 20 ns constant pH molecular dynamics simulations of chitinase I at a pH range 2–6 in a solvent. This work was aimed at establishing the optimum activity and stability profiles of chitinase I. We observed a strong conformational pH dependence of chitinase I and the enzyme retained their characteristic TIM barrel topology at low pH.

## 1. Introduction

The thermostable nature of chitinase isolated from thermophilic organisms like *Thermomyces lanuginosus* has been the primary focus of research in the past few years mainly due to their important bio-physiological functions and applications, ranging from biocontrol of fungal phytopathogens [1,2] to chemical fungicides owed to their natural stability at elevated temperatures and broad pH range.[3,4] Chitinases are a class of enzymes that hydrolyse the chitins, a naturally occurring polysaccharide that have a linear polymer of β (14) N-acetyl β-D-glucosamine.[5] Chitinases are present in all forms of life such as plants, bacteria, animals, fungi and viruses. They form a set of extremely conserved enzymes that display diverse roles in these creatures. These enzymes possess a peculiar capability to hydrolyse the insoluble chitin polymer to the lower molecular weight chito-oligomers, which are used in agricultural, industrial, biotechnological and medical fields.[6,7]

Chitinases from fungal source mainly belong to the 18 glycosyl hydrolases family, and exhibit a higher amino acid similarity with class III plant chitinases.[8] The 18 glycosyl hydrolases chitinase family contains 5 domains that are catalytic domain, signal peptide at N-terminal region, serine/threonine rich region, chitinbinding site and Cterminal extension region. The N-terminus signal peptide is an indicator of the protein secretion that targets the protein outside the cells through secretory pathways. The catalytic domain is responsible for the hydrolysis

of chitin, and is the most important domain of this chitinase. The family G18 chitinases have two highly conserved motifs such as $D_{XX}D_XD_XE$ and $S_XGG$, corresponding to the catalytic domains and substrate-binding sites, respectively.[9] The highly conserved Glu (E) and Asp (D) residues in the catalytic domains suggesting their contribution to the hydrolysis of glycosidic bond.

Chitinases have various tasks in morphogenesis, nutrition, defence and development processes in fungi. Fungal chitinases are also involved in the improvement of resistance in plant by genetic manipulations. Chitinases are used in pollution treatment, pest and mosquito control, and biocontrol applications. Chitinases also play a significant role in single-cell protein production, fungal protoplast generation, bioactive chito-oligosaccharides preparations and shellfish waste degradation. [10] However, regardless of their vast applications, the three-dimensional (3D) structure of chitinase from *T. lanuginosus* is not completely characterised.[11] In this study, homology modeling techniques were utilised to generate a 3D structure of chitinase I in the absence of an experimentally determined structure.[12] The generated structure was subjected to energy minimisation and refinement. The top model was further subjected to molecular dynamics (MD) simulations at 300–375 K to understand the physical basis of the structure and conformations. MD simulations of protein provide comprehensive information on the fluctuations and conformational changes during the time scale.

---

**CONTACT** Dong-Qing Wei ✉ dqwei@sjtu.edu.cn

[13,14] Furthermore, the MD simulations at constant pH offer a profound insight into the structural and functional features of the enzyme molecule.[15] A recently developed constant pH MD simulation techniques directly captured the protonation of residues, thereby increasing the realism of MD simulations as potential tools.[16–18] Accordingly, in this study, the MD simulations were also performed with a fixed protonation state of the enzyme. The pKa values of the titratable groups were obtained by modulating the protonation states of the various titratable functional groups present in the system.[19] The prime objective of this study was to evaluate the effect of the physiological pH and temperatures on chitinase I enzyme obtained from *T. lanuginosus* SSBP. To the best of my knowledge, MD simulations at constant pH and wide range of temperatures on thermostable chitinase I were performed for the first time. The results suggested a strong temperature and pH dependence on the conformation of chitinase I enzyme.

## 2. Materials and methods

### 2.1. Sequence analysis

The 400 long residues for the amino acid sequence of chitinase I from *T. lanuginosus* SSBP were submitted in the NCBI (Accession: AIW06013) and evaluated using BLAST [20], FASTA server [21] and HMMER [22]. The InterProScan 5 [23], SMART [24], SYSTERS [24] and ProtoNet [25] were used for domain analysis. The PTM code [26] was employed to identify any potential post-translational modification sites present in the protein sequence of chitinase I. The Psipred [27] were used to analyse sequence based secondary structure. The artificial neural network algorithm-based SignalP 4.0 [28] were used to detect the presence of signal peptide in the sequence framework of chitinase I. Protein glycosylation is significant for secretion, localisation and stability of protein. Thus, the glycosylation site was predicted using NetNGlyc 1.0 Server.

### 2.2. Structure prediction and analysis

Chitinase I structure was predicted using homology modelling techniques. The suitable template search was carried out in the pProtein data bank (PDB) [29] using PSI-BLAST, HHpred [30], HMMER [22] and Phyre [31]. The BLAST [20] search with identity (>30%) was regarded as the appropriate template for the structure prediction of chitinase I. HHpred module identified structural homologs in the PDB, while HMMER module was used to detect reliable homologs in the databases using modules such as hmmsearch, hmmscan, jackhammer and phemmer. Similarly, Phyre, a server based on profile–profile matching algorithm was used to enhance the accuracy of the similarity search. The fold recognition methods were used to optimise the sequence-structure alignment, which was further utilised to develop the three-dimensional models using MODELLER 9.15 [32]. The homology modelling is based on the alignments with known proteins. The best models were assessed on the basis of TM score, RMSD and DOPE Profile. The top models were further subjected to refinements using SCWRL 4.0 [33] and CHARMm [34] energy minimisation using ChiRotor algorithm of Discovery Studio 4.0. The computational servers such as VERIFY3D [35],

PROCHECK [36] and ERRAT [37] were used for the evaluation of generated models. The residues which are present in active pockets were predicted by metaPocket 2.0 [38], COFACTOR [39] and COACH [40] server. The metaPocket 2.0 algorithm uses PASS, LIGSITEcs, SURFNET, Q-SiteFinder, GHECOM, Fpocket, ConCavity and POCASA algorithms to identify the active pockets. The COFACTOR identifies the template proteins with similar folds and functional sites by threading the target structures through three representative template libraries, with known protein–ligand binding interactions and enzyme commission number or gene ontology terms. The COACH server was based on TM-SITE and S-SITE for complementary binding site predictions. The docking studies were further performed with chitinase inhibitors acetazolamide, allosamidine and allosamizoline as ligands,[41] using AutoDock to visualise the interaction with the predicted active pocket site. Gasteiger charges were added and the nonpolar hydrogen atoms were merged to carbon atoms in all the ligand structures. The ligands were docked into the binding site of chitinase I protein by defining the grid size of $70 \times 70 \times 70$ pointing in $x$, $y$ and $z$ directions around the active site. Ten conformations were generated for each docked ligand and the best pose with the lowest docked binding energy was selected for analysis.

### 2.3. Constant-temperature MD simulations

Several significant biological roles of proteins and dynamic mechanisms were discovered by looking at their internal motions. [42,43] MD simulations track the behaviour of system and are helpful to study the protein folding.[44,45] These methods are used to investigate the structure, dynamics and thermodynamics of biological molecules. The MD simulations were performed by GROMACS 4.6.5 [46], and all atom functions by optimised potential for liquid simulation (OPLS). The OPLS-AA (all atom) force field consists of a series of modifications of torsional parameters incorporated into the *ab initio* results [47] used in the prediction of side-chain rotamer preferences, which are critical for accurate protein homology modelling protocols. The OPLS-AA force field incorporated in the GROMACS simulation package includes all atoms explicitly modelled and designed to reproduce experimental properties. MD simulation methods were performed on chitinase I at four different temperatures 300, 325, 350 and 375 K, to study its stability profile. Chitinase I was immersed in a box of water molecules with a cubic dimension of 10 Å, using *editconf* module for creating boundary conditions and *genbox* for solvation. The spc216 water template was used in this step. Overall neutrality of the system was ensured by adding counterions $Na^+$ and/or $Cl^-$ using the verlet cut off scheme. The whole system was then minimised so as to combat improper geometry and structure deformation using 1500 steps of steepest descent methods until a maximum force (<1000 kJ/mol/nm) was obtained. For each system, the temperatures were subsequently increased from 0 to 300–375 K during their equilibration period (100 ps) under periodic boundary conditions. The equilibration was attained in two sets of *NVT* (constant number of particles, volume and temperature ensemble), and *NPT* (constant number of particles, pressure and temperature ensemble), followed by the production phase of 10 ns at 300, 325, 350 and 375 K.

The outcomes were examined using *g_rms*, *g_rmsf*, *g_gyrate* and *do_dssp* utilities of GROMACS. The results were generated using GRACE (GRaphing Advanced Computation and Exploration of data) plotting tool. All the pictorial presentations were prepared using Visual Molecular Dynamics.[48]

### 2.4. Protein ionisation and pKa calculations

pKa values of the amino acid side chains aid in defining the pH-dependent characteristics of a protein.[49] The pH-dependent protein stability and activity exhibited by enzymes determined by the pKa values of amino acid side chains. The combination of the generalised born (GB),[50] and iterative mobile clustering (IMC) [51] approaches provided new computational protocols for pKa calculations.[52] The pKa value and titration curves for every titratable amino acid residues present in chitinase I was computed using Discovery studio 4.0 [52]. On the other hand, CHARMm (Chemistry at HARvard Molecular Mechanics) is a highly versatile and widely used molecular simulation programme that primarily focuses on biological molecules such as proteins and peptides. The structures for chitinase I was prepared using the CHARMm polar hydrogen force field. The total charge, isoelectric points (pI) and electrostatic contribution to the free energy as a function of pH were calculated for chitinase I molecule. The method is implemented as a computational protocol 'Protein Ionization and residual pK' in Accelrys Discovery Studio and provides a fast and easy way to study the effect of pH on many important mechanisms such as enzyme catalysis, ligand binding, protein–protein interactions and protein stability. This information is utilised for precipitation and purification of protein. Protein at pH equals pI tends to precipitate due to the absence of net charge on the surface. This leads to reduced solubility because the protein is unable to interact with the medium.

### 2.5. Constant pH MD simulations

pH determines the charges of the ionisable residues, reveals a direct influence on the intra-molecular electrostatic interactions thereby influencing the molecular structure.[53] The pH-dependent protein stability is a critical factor for protein folding which is a key to various molecular mechanisms. In protein folding, the titratable amino acids in the proteins are modified, depending upon the nature of the buried amino acids with no exposure to the solvent. Specifically, pKa values of the amino acid side chains play a pivotal role in defining the pH-dependent characteristics of a protein.[54] Literature studies revealed that
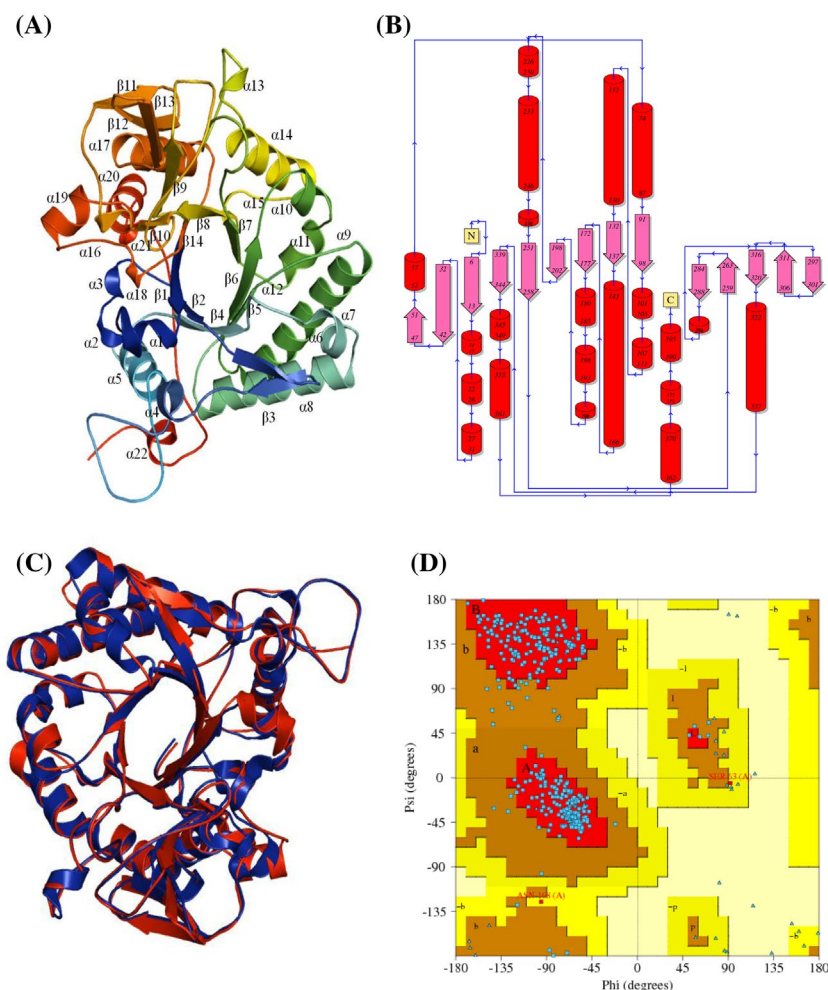


**Figure 1.** (Colour online) (A) The predicted 3D structure of chitinase I indicating the characteristic TIM barrel present in the framework, (B) topology map generated by PDB sum indicating 22 helices with 16 helix–helix interactions as well as 4 beta–alpha–beta motifs present in the structure of chitinase I, (C) overlay of the predicted model of chitinase I (red) and template (blue) with obtained RMSD values of 0.303 Å. All atoms of proteins are represented in cartoon form, and (D) the Ramachandran plot of predicted chitinase I indicating total residues in the most favoured regions and additional allowed regions are 90.7 and 8.7%, respectively.

**Table 1.** The obtained binding energies and the residues involved in the interactions with chitinase I active site when docked with acetazolamide, allosamidine and allosamizoline, respectively.

| S. No. | Inhibitors | Binding Energy (kcal/mol) | Residues involved |
|---|---|---|---|
| 1 | Acetazolamide | −7.24 | Glu139, Tyr140, Ala179,Met202, Tyr204, Asp205 |
| 2 | Allosamidine | −4.97 | Trp99, Thr100, Glu139, Ala179, Met202, Tyr204, Asp205, Tyr259, Trp344 |
| 3 | Allosamizoline | −6.45 | Glu139, Tyr140, Asn183, Tyr204, Asp205, Tyr206, Phe232 |

pH has a dramatic impact on biomolecules.[55,56] The constant pH MD simulation method was implemented in the GROMACS package developed by Baptista and co-workers [57]. The protonation was carried out via *pdb2gmx* component of GROMACS by utilising the information obtained from Discovery Studio.[46] The protonation of residues present in the chitinase I is done by using –*ter* and –*inter* flag, interactively. The obtained information of protonating residues at desire pH was carried out at a range of pH 2–6 each at 20 ns MD simulations using same methodology mentioned above.

## 3. Results and discussion

### 3.1. Sequence analysis

The ProtParam [58] revealed that chitinase I DNA encodes a 400 amino acid protein of molecular weight 44.14 KDa and theoretical pI of 5.64. The half-life of chitinase I was predicted to be more than 20 h in yeast. The HMMER and FASTA results indicated the query containing chitinase-like activity. The InterProScan

suggested that chitinase I domains are similar to the glycoside hydrolase family 18. Similarly, SMART characterised the query protein to be an o-glycosyl hydrolase. The query protein also belonged to 4,164,978 and 136,700 clusters of ProtoNet and SYSTERS groups of chitinase-like enzymes with α-β barrel architecture, respectively. The presence of two N-linked glycosylation site occupied by Asparagine at positions 67 and 183 was predicted. The secondary structure topology predicted by the PSIPRED server suggested that the chitinase I may consist of 8 helices and 12 β-strands connected via loops.

### 3.2. Structure prediction and analysis

Analysis of the sequence similarity searches showed the chitinase-like activities in the structure framework. Chitnase I is related to *Aspergillus fumigatus* chitinase (PDB ID: 1WNO) with 62% identity selected as an appropriate template for structure prediction. The MODELLER 9.15 aligned the query sequence with the template structure which thereafter predicted the structure by satisfying the spatial restraints. The predicted structure of chitinase I showed low violations of the restraints. Accordingly, 10 3D models were generated, and selected on the basis of DOPE profile, molecular probability density function (Mol PDF), RMSD and TM-score. The final model showed overhanging sequences which were further modelled using *ab intio* protocols of the I-TASSER [59] and ROBETTA [60] servers. The generated structures and topology of the chitinase I are shown in Figure 1. The topology for the chitinase I was created by PDBsum in order to get the detailed structural information.[61] The DOPE score for chitinase I and its template (PDB: 1WNO) were −41,595.5585 and −49,313.0078, respectively. This indicated the reliability of
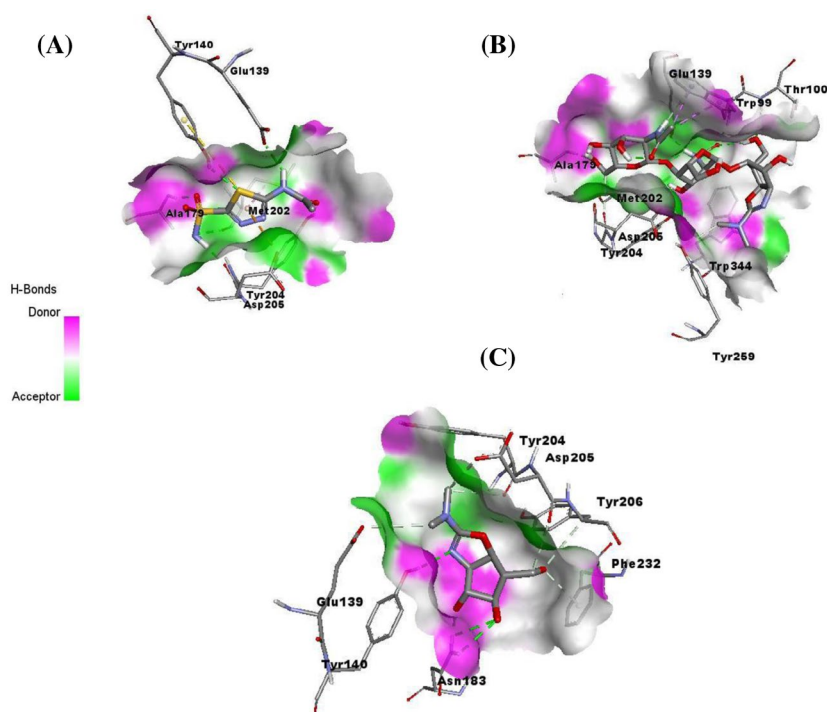


**Figure 2.** (Colour online) Possible docked positions of chitinase I using (A) acetazolamide, (B) allosamidin, and (C) allosamizoline inhibitors as ligands, indicating the residues present in active pocket of chitinase I.

the predicted models, which were subjected to further optimisation and refinement. The side chains of the chitinase I were refined with the SCWRL4. The energy minimisations of the 3-D structures were performed in order to shun bad molecular interactions. The resulting chitinase I models showed a minimised energy of −9060.353 kJ/mol. The RMSD and TM scores between the chitinase I and its template (PDB: 1WNO) were 0.303 and 0.7148 Å, respectively, indicating a high similarity of the structures. The models were further evaluated using PROCHECK, which showed 90.7% of the total residues in the most favoured regions, 8.7% in the additional allowed regions and 0% in disallowed regions of the Ramachandran Plot. On the other hand, the template showed 90.2% of the total residues in the most favoured regions, 8.6% in the additional allowed regions and 0.3% in the disallowed regions. Verify_3D showed 98% of the total residues had an normal 3D–1D score (>0.2) signifying the consistency of the model prediction. The overall quality factor score predicted by Errat was 96.4. The topology of chitinase I confirmed trans-glycosidases like α/β TIM-barrel with 18.8% β-strand, 27.2% α-helix and 7.5% 3–10 helix. The chitinase I structure have two β sheets with five anti parallel β-strands and nine mixed β-strands. There were 22 helices, 16 helix–helix interactions and 4 β–α–β motifs. The template used for the structure prediction also consists of 2 β sheets with 5 anti-parallel β-strands, 9 mixed β-strands, 16 helix–helix interactions, 4 β–α–β units and 21 helices. The similarity in the topology of template and 3D model of chitinase I suggested the reliability of structural prediction.

### 3.3. Active site prediction and docking study

The results obtained from the metaPocket 2.0, COFACTOR and COACH servers suggested that the active pocket of the chitinase I may contain Tyr10, Phe38, Asp135, Asp137, Glu139, Met202, Tyr204, Asp205, Tyr259 and Trp344 amino acid residues. In order to validate the above predicted results docking analysis were performed using AutoDock. Acetazolamide, allosamidine and allosamizoline bind with the residues Trp99, Thr100, Glu139, Tyr140, Ala179, Asn183, Met202, Tyr204, Asp205, Tyr206, Phe232, Tyr259 and Trp344 (Table 1). The best docked structures represented in Figure 2 clearly shows that the residues
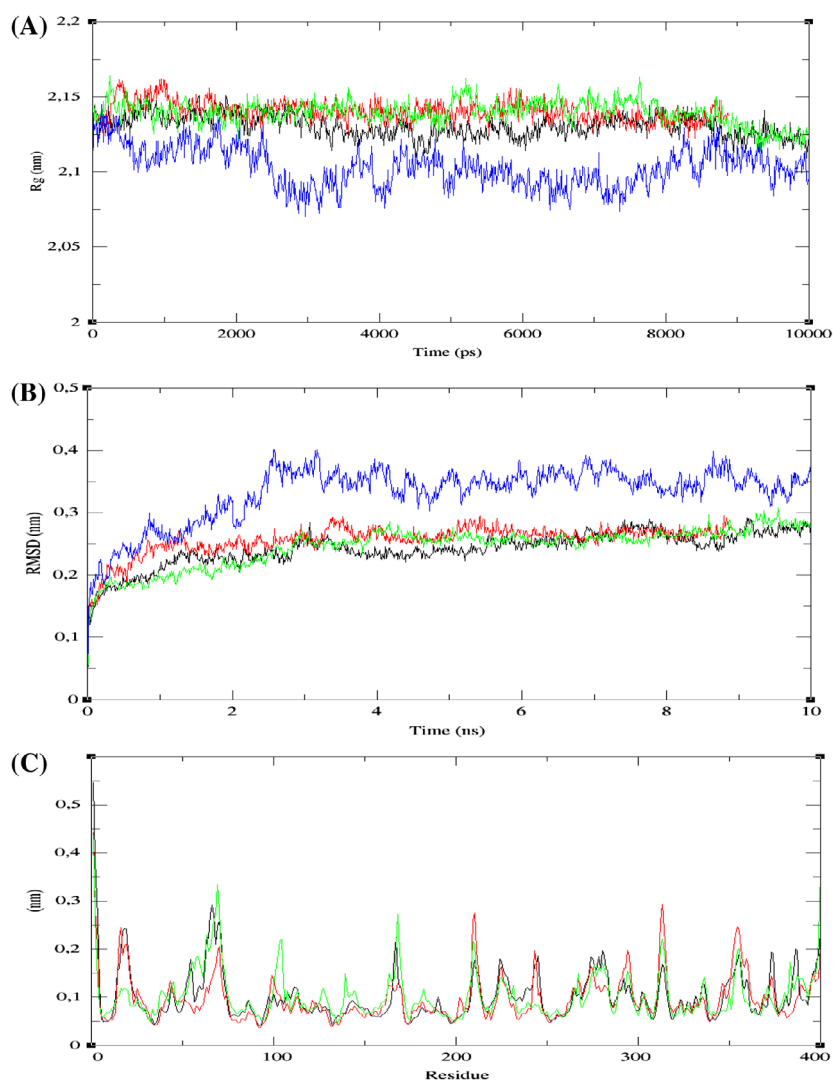


**Figure 3.** (Colour online) (A) The radius of gyration, (B) average RMS deviation and (C) average RMS fluctuation values for chitinase I. Black, red, green and blue represent the calculations obtained at 300, 325, 350 and 375 K, respectively.

Glu139, Met202, Tyr204, Asp205, Tyr259 and Trp344 of chitinase I are actively involved in binding with the inhibitors. Literature studies revealed that allosamidin is a broad-spectrum inhibitor, inhibiting all characterised family 18 chitinases. It is used as a pharmacophore for the development of novel compound.[62] It has been shown that allosamidin and its derivatives bind to the active pocket of chitinases that lead to a distortion of the conformations.[63] Literature studies also revealed that allosamidin is less efficient as an inhibitor for *A. fumigates* chitinase as compared to acetazolamide and 8-chlorotheophylline due to large size.[64]

### 3.4. Temperature effect on the overall structure

The thermodynamic properties such as average temperature and total energy values were performed to assess the quality of the MD simulations. The stable regular fluctuation of temperature for each system around 300, 325, 350 and 375 K, respectively, indicated accurately as well stabled and nature of the MD simulations was carried out. The radius of gyration (Rg) of a protein is a measure of its compactness.[65] Here, the analysis provides the overall dimension or compactness of the protein. If a protein is folded in a stable configuration, it will then likely to maintain a relatively steady value of Rg. The calculated average Rg values ranged from 2.10 to 2.15 nm. The Rg values at 300–350 K

were found to be constant and comparable, while Rg values at 375 K showed different values with higher fluctuations observed throughout the simulations. The Rg plot indicated that chitinase I acquired its compact (folded) and stable form at a temperature range of 300–350 K, with the absence of compactness observed at 375 K (Figure 3(A)). Amongst same-sized proteins, the α/β proteins have a larger contacts per residue due to compact and globular structure.[65] On the other hand, the hydrophobic interactions play an important role in protein folding. So, the higher hydrophobicity could result in additional packed conformations due to strong solvent pressure. At higher temperature, the hydrophobicity of a protein loses and the solvent pressure decreases, thus the compactness of chitinase I is not maintained at 375 K. The protein with α/β motifs has slowest folding kinetics and the largest number of residual contacts.[66] So, the α/β pattern in the chitinase I may contribute to its compactness even at 350 K.

Measures of structural similarity between proteins are a valuable tool for the examination of protein folding during simulations. Root mean square deviation (RMSD) is an essential property to establish whether the given structure is stable and similar to its experimental structure.[67] The RMSD is a measure of the deviation in the conformational stability of the proteins from the backbone structure to the initial starting structure. The RMSD values were found to be constant around 0.25 nm for
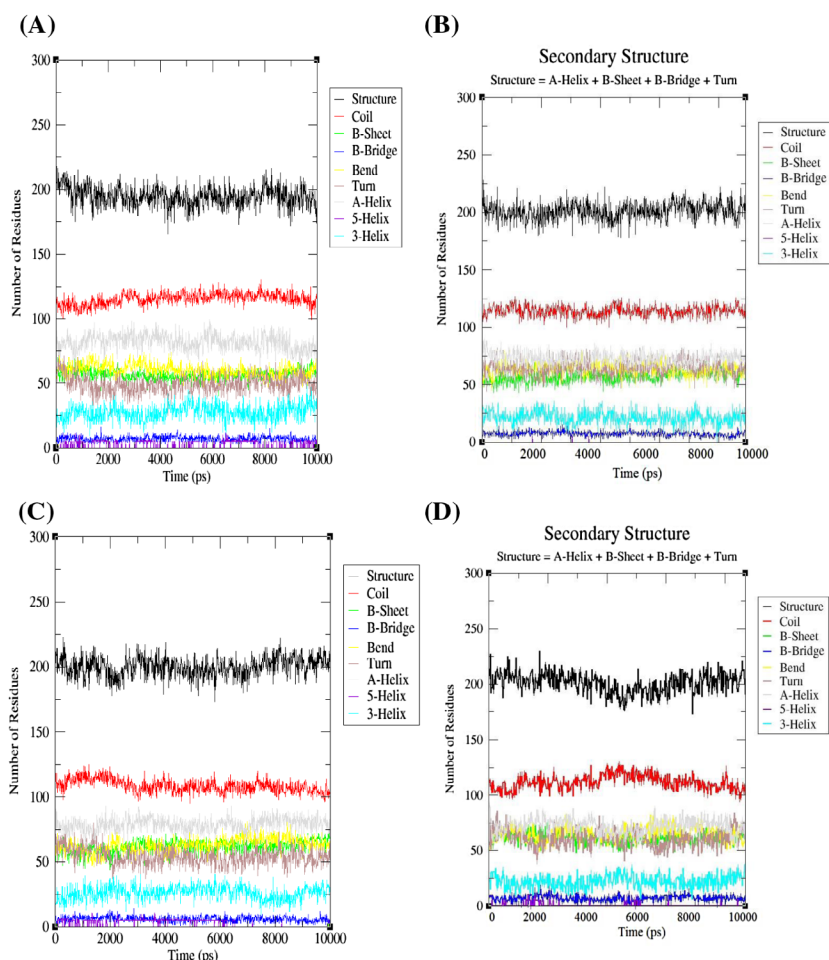


**Figure 4.** (Colour online) Graphical representation indicating the stability of structural elements of chitinase I at (A) 300 K, (B) 325 K, (C) 350 K and (D) 375 K, respectively.

temperatures ranging from 300 to 350 K, while a higher value (0.4 nm) with fluctuations observed at 375 K as depicted in the plots (Figure 3(B)). The average RMSD values of the chitinase I structure were found to be lower at 350 K than at 325 K. This clearly indicates that the chitinase I acquired its stable conformations even at 350 K. Increase in RMSD at 375 K suggested that chitinase I undergo unfolding. Observing the RMSD of given protein structure provides insights into structural conformation during MD simulations. At 300–350 K, the fluctuations in the RMSD value to the end of the simulation are roughly at some thermal average structure that suggests that the simulation has been equilibrated. Changes in the order of 0.25 nm at 300–350 K are perfectly acceptable while much larger (0.4 nm) at 375 K signifies that the protein structure gone through a large conformational distortions.

Vibrations around the equilibrium depend on local structure flexibility. It has been shown that protein backbone fluctuations are evolutionarily conserved.[68] The average fluctuation of residues present in chitinase I was calculated using root mean square fluctuation (RMSF).[67] The RMSF is a measure of deviation between the position of a particle and some reference position. Here, the RMSF of the Cα value was comparable for all temperatures with minor fluctuations observed at 350 K (Figure 3(C)).

The secondary structures obtained during the MD simulations are depicted in Figure 4. The purpose of this analysis is to measure the secondary structure content of a protein as a function of time. The secondary structure assignments such as helix, sheet and turn were broken into individual residues for each time step to quantify the data in meaningful ways. Results obtained from secondary structure analysis clearly suggested that the global TIM-Barrel conformation of chitinase I is conserved with no significant changes in its secondary structure elements.

### 3.5. Protein ionisation and pKa measurements

The total titration curve of chitinase I obtained by computing the average net charge with respect to pH value (Figure 5(A)). The net charge and isoelectric pH (pI) of a protein depend on the content of ionisable groups and their pKa values. The maximum stability of chitinase I was obtained at pH 3.6 and 2.2 using CHARMm and CHARMm Polar H force fields, respectively (Figure 5(B)), and the corresponding isoelectric points of 6.08 and 4.35, respectively (Table 2). The total charge at a particular pH was lower than those computed using CHARMm Polar H force fields, while the relative folding energies were lower than those computed using CHARMm force fields. Electrostatic interactions are widely believed to be primary factors relating to the pH-dependent phenomena. Since the charges carried by proteins are pH-dependent, the electrostatic interactions between residues of the proteins would be modulated by pHs. The electrostatic energy of chitinase I was found to be less at lower pHs, indicating that chitinase I are stable at low pH [69] (Figure 5(C)). The required protonation conditions are produced by modifying the configuration of the amino acids using *pdb2gmx* module present in GROMACS. Within the protein, the individual titratable residues were picked on the basis of information achieved from titration analysis. It was observed that chitinases attained a more stable conformation at a lower pH over the 20 ns simulations.
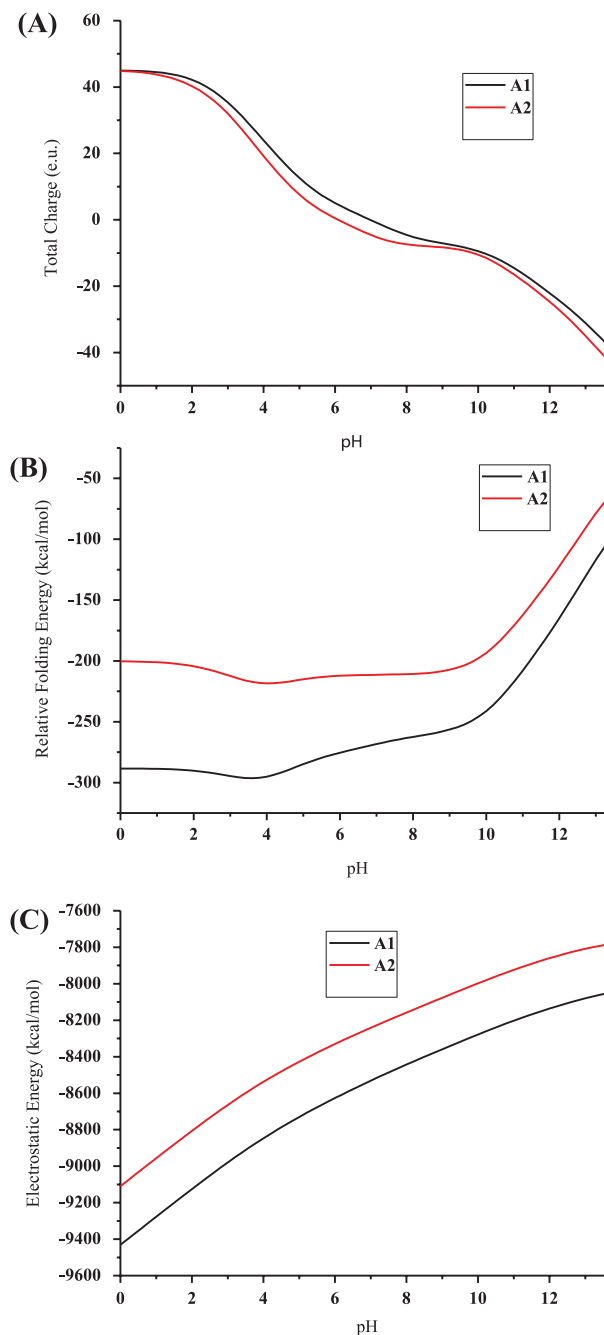


**Figure 5.** (Colour online) (A) The pH dependence of total charge, (B) relative folding energy and (C) electrostatic energy obtained for chitinase I at different protonated states. A1 and A2 represent CHARMm and CHARMm Polar H force fields, respectively.

### 3.6. pH effect on the overall structure

Chitinase I showed a low value of average total energy of −1,011,618 kK/mol at pH 5. By considering the radius of gyration (Rg), we can conclude that Chitinase I remained in its compact state at pH 2, 3, 5 and 6, while it loses its compactness after 10 ns at pH 4 (Figure 6(A)). Chitinase I has least average RMSD value at pH 3 (0.16 nm), pH 5 (0.17 nm) and pH 6 (0.16 nm). The values were found to be constant and stable throughout the time scale at pH 5, indicating that chitinase I is highly stable at pH 5 (Figure 6(B)). Additionally, more flexible regions were identified

**Table 2.** Folding energy, Isoelectric point and electrostatic energy of chitinase I obtained using CHARMm and CHARMm Polar H force-fields.

| Force-field | Chitinase I | |
| --- | --- | --- |
| | CHARMm | CHARMm Polar H |
| Maximum stability at pH | 3.6 | 4 |
| Isoelectric point | 6.98 | 6.08 |
| Electrostatic energy (kcal/mol) | −7962.0 | −7728.8 |

by RMSF plot for the protonated enzyme during simulations. Our results clearly showed that chitinase I with a lower average RMSF value at pH 5 and pH 6, but with higher deviations in the α-helical regions of residues 50–60 were observed at pH 3 (Figure 6(C)). However, for residues between 40 and 70, higher and unstable fluctuations were observed at pH 4. The RMSF values for most of the residues were below 0.1 nm, indicating the stable nature of chitinase I at pH 5. The average structures at each pH suggested that the TIM-Barrel conformation of chitinases was maintained during the 20 ns simulations. The RMS

deviations of native and simulated structures of chitinase I were found to be 1.174, 1.134, 1.359, 1.065 and 1.277 Å (Figure 7) at pH 2–6, respectively. The lowest RMS deviations for chitinase I were observed at pH 5. The above data suggest that the optimum pH for chitinase I was observed at 5. The number of internal hydrogen bonds varied for corresponding changes in pH. The average number of hydrogen bonds between main chain and side chains of chitinase I was found to be comparable at pH 3 (45) and pH 5 (44), indicating the stable folding, while fewer hydrogen bonds were observed at pH 2, 4 and 6, respectively.

## 4. Conclusions

The present research work offer insights into the structural and dynamical aspect of a chitinase I isolated from *T. lanuginosus*. The three-dimensional structure of chitinase I was generated with high accuracy using various available prediction algorithms. These models showed high structure similarities to the
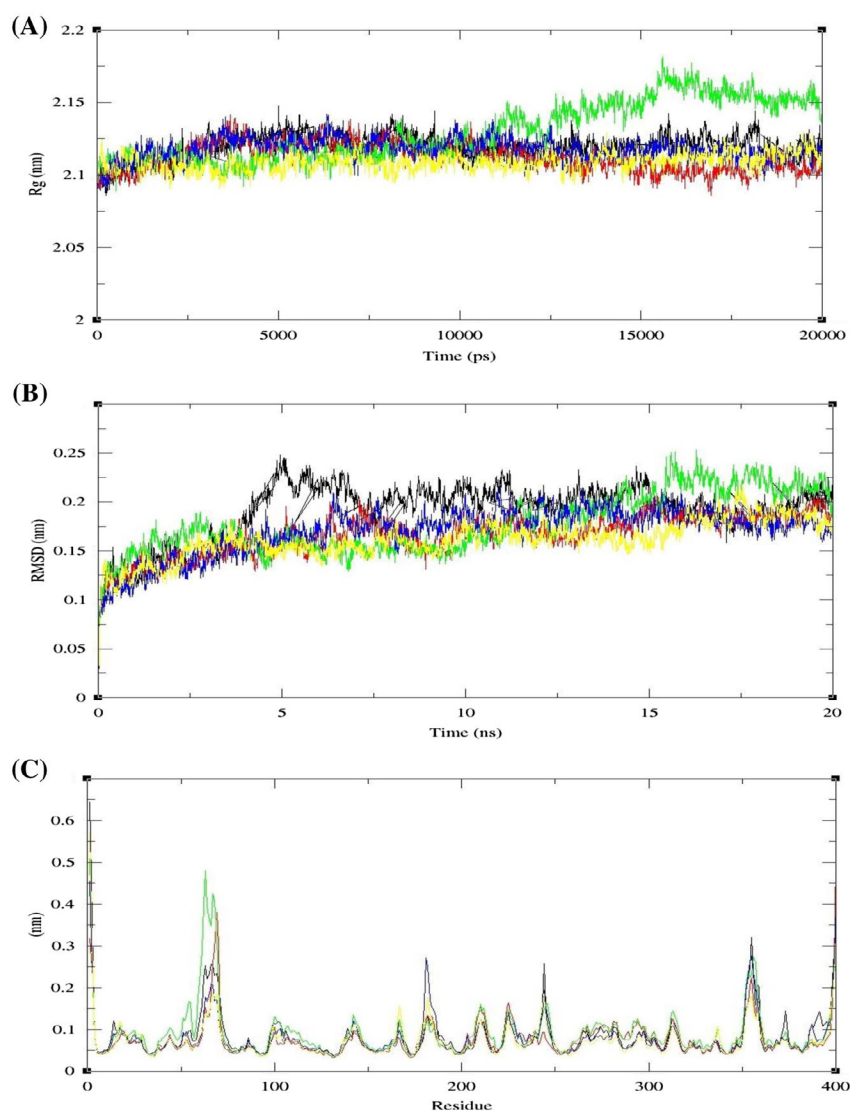


**Figure 6.** (Colour online) (A) The radius of gyration, (B) RMS deviation and (C) average RMS fluctuations obtained for chitinase I. Black, red, green, blue and yellow colour represent the calculations obtained at pH 2, 3, 4, 5 and 6, respectively.
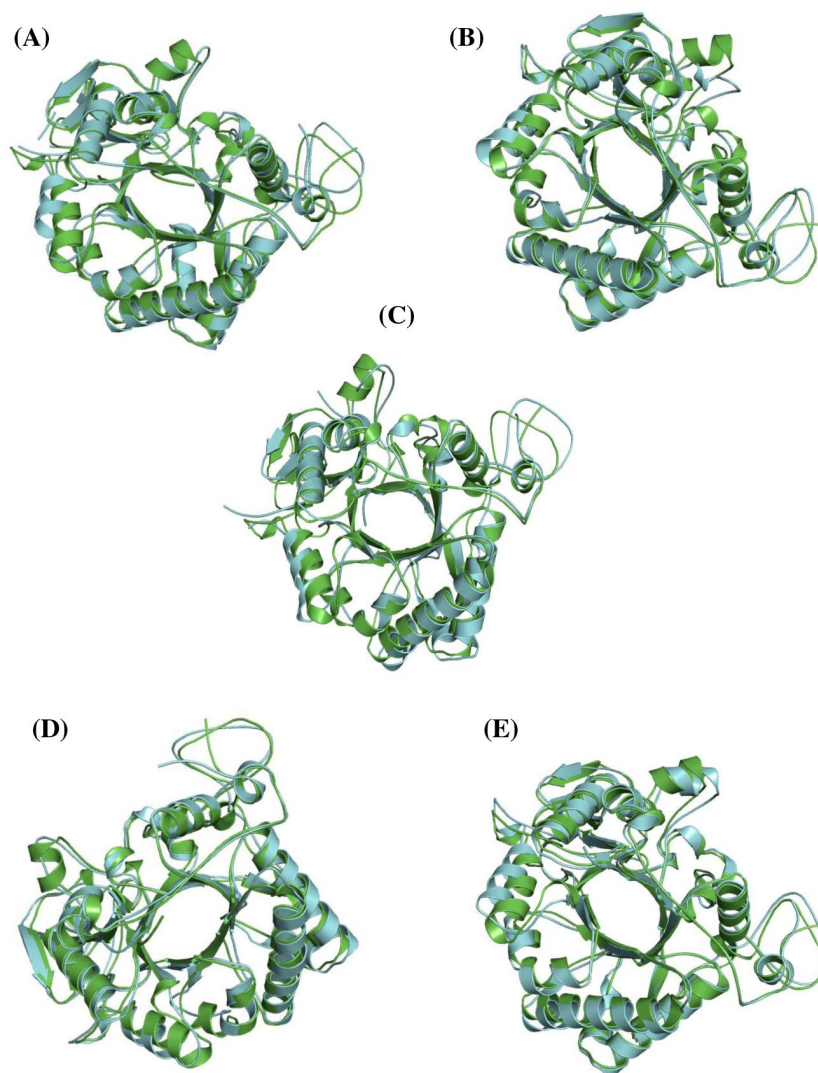
**(A)**

**(B)**

**(C)**

**(D)**

**(E)**

**Figure 7.** (Colour online) The superimposition of native and simulated structures of chitinase I at pH 2, 3, 4, 5 and 6. Green and blue represents the native and the simulated chitinase I structures, respectively. The RMS deviations were found to be 1.174, 1.134, 1.359, 1.065 and 1.277 Å, respectively.

chitinase-like proteins with the characteristic $(\alpha/\beta)_8$ TIM barrel conformations. The structure of chitinase I enzyme was found to be compact due to the hydrophobic interactions with the surrounding water molecules, the hydrogen bonding between the amino acid residues and the formation of a core by the combination of several secondary structure elements. The structural effects arising from temperature and pH-induced changes on chitinase I enzyme has been performed using molecular dynamics simulations method. We also presented a titration curve and pK calculations of the titratable residues at a particular pH. Our results suggested that the maximum stability and optimal activity of chitnase I favours an acidic pH. The chitinase I remained in their close TIM barrel conformations during the MD simulations.

## Funding

## ORCiD

*Faez Iqbal Khan* 🆔 http://orcid.org/0000-0001-9088-0723
*Md. Imtaiyaz Hassan* 🆔 http://orcid.org/0000-0002-3663-4940

## Conflict of interest

The authors have no substantial financial or commercial conflicts of interest with the current work or its publication.

## References

[1] Hamid R, Khan MA, Ahmad M, et al. Chitinases: an update. J. Pharm. Bioallied Sci. 2013;5:21–29.
[2] Singh S, Madlala AM, Prior BA. Thermomyces lanuginosus: properties of strains and their hemicellulases. FEMS Microbiol. Rev. 2003;27:3–16.
[3] Herrera-Estrella A, Chet I. Chitinases in biological control. EXS. 1999;87:171–184.
[4] Maheshwari R, Bharadwaj G, Bhat MK. Thermophilic fungi: their physiology and enzymes. Microbiol. Mol. Biol. Rev. 2000;64:461–488.
[5] Henrissat B. Classification of chitinases modules. EXS. 1999;87:137–156.

[6] Bucolo C, Musumeci M, Musumeci S, et al. Acidic Mammalian chitinase and the eye: implications for ocular inflammatory diseases. Front. Pharmacol.. 2011;2:43. doi:http://dx.doi.org/10.3389/fphar.2011.00043.

[7] Lobo MD, Silva FD, Landim PG, et al. Expression and efficient secretion of a functional chitinase from *Chromobacterium violaceum* in *Escherichia coli*. BMC Biotechnol. 2013;13:1–15. doi: http://dx.doi.org/10.1186/1472-6750-13-46.

[8] Hayes CK, Klemsdal S, Lorito M, et al. Isolation and sequence of an endochitinase-encoding gene from a cDNA library of *Trichoderma harzianum*. Gene. 1994;138:143–148.

[9] Henrissat B, Bairoch A. Updating the sequence-based classification of glycosyl hydrolases. Biochem. J. 1996;316:695–696.

[10] Khan FI, Bisetty K, Singh S, et al. Chitinase from *Thermomyces lanuginosus* SSBP and its biotechnological applications. Extremophiles. 2015;19:1055–1066.

[11] Khan FI, Govender A, Permaul K, et al. Thermostable chitinase II from *Thermomyces lanuginosus* SSBP: cloning, structure prediction and molecular dynamics simulations. J. Theor. Biol. 2015;374:107–114.

[12] Wiltgen M, Tilz GP. Homology modelling: a review about the method on hand of the diabetic antigen GAD 65 structure prediction. Wien. Med. Wochenschr. 2009;159:112–125.

[13] Gramany V, Khan FI, Govender A, et al. Cloning, expression, and molecular dynamics simulations of a xylosidase obtained from *Thermomyces lanuginosus*. J. Biomol. Struct. Dyn. 2015;34:1–12.

[14] Khan FI, Wei DQ, Gu KR, et al. Current updates on computer aided protein modeling and designing. Int. J. Biol. Macromol. 2016;85:48–62.

[15] Kim MO, Blachly PG, Kaus JW, et al. Protocols utilizing constant pH molecular dynamics to compute pH-dependent binding free energies. J. Phys. Chem. B. 2014.

[16] Chen W, Morrow BH, Shi C, et al. Recent development and application of constant pH molecular dynamics. Mol. Simul. 2014;40:830–838.

[17] Goh GB, Knight JL, Brooks CL 3rd. Constant pH molecular dynamics simulations of nucleic acids in explicit solvent. J. Chem. Theor. Comput. 2012;8:36–46.

[18] Machuqueiro M, Baptista AM. Constant-pH molecular dynamics with ionic strength effects: protonation-conformation coupling in decalysine. J. Phys. Chem. B. 2006;110:2927–2933.

[19] Burgi R, Kollman PA, van Gunsteren WF. Simulating proteins at constant pH: an approach combining molecular dynamics and Monte Carlo simulation. Proteins. 2002;47:469–480.

[20] Altschul SF, Gish W, Miller W, et al. Basic local alignment search tool. J. Mol. Biol. 1990;215:403–410.

[21] Pearson WR, Lipman DJ. Improved tools for biological sequence comparison. Proc. Natl. Acad. Sci. U.S.A. 1988;85:2444–2448.

[22] Finn RD, Clements J, Eddy SR. HMMER web server: interactive sequence similarity searching. Nucleic Acids Res. 2011;39:W29–W37.

[23] Jones P, Binns D, Chang HY, et al. InterProScan 5: genome-scale protein function classification. Bioinformatics. 2014;30:1236–1240.

[24] Schultz J, Copley RR, Doerks T, et al. SMART: a web-based tool for the study of genetically mobile domains. Nucleic Acids Res. 2000;28:231–234.

[25] Rappoport N, Karsenty S, Stern A, et al. ProtoNet 6.0: organizing 10 million protein sequences in a compact hierarchical family tree. Nucleic Acids Res. 2012;40:D313–D320.

[26] Minguez P, Letunic I, Parca L, et al. PTMcode: a database of known and predicted functional associations between post-translational modifications in proteins. Nucleic Acids Res. 2013;41:D306–D311.

[27] McGuffin LJ, Bryson K, Jones DT. The PSIPRED protein structure prediction server. Bioinformatics. 2000;16:404–405.

[28] Petersen TN, Brunak S, von Heijne G, et al. SignalP 4.0: discriminating signal peptides from transmembrane regions. Nat. Methods. 2011;8:785–786.

[29] Berman HM, Westbrook J, Feng Z, et al. The protein data bank. Nucleic Acids Res. 2000;28:235–242.

[30] Soding J, Biegert A, Lupas AN. The HHpred interactive server for protein homology detection and structure prediction. Nucleic Acids Res. 2005;33:W244–W248.

[31] Kelley LA, Sternberg MJ. Protein structure prediction on the Web: a case study using the Phyre server. Nat. Protoc. 2009;4:363–371.

[32] Eswar N, Eramian D, Webb B, et al. Protein structure modeling with MODELLER. Methods Mol. Biol. 2008;426:145–159.

[33] Wang Q, Canutescu AA, Dunbrack RL Jr. SCWRL and MolIDE: computer programs for side-chain conformation prediction and homology modeling. Nat. Protoc. 2008;3:1832–1847.

[34] Vanommeslaeghe K, Hatcher E, Acharya C, et al. CHARMM general force field: a force field for drug-like molecules compatible with the CHARMM all-atom additive biological force fields. J. Comput. Chem. 2010;31:671–690.

[35] Luthy R, Bowie JU, Eisenberg D. Assessment of protein models with three-dimensional profiles. Nature. 1992;356:83–85.

[36] Laskowski RA, Rullmannn JA, MacArthur MW, et al. AQUA and PROCHECK-NMR: programs for checking the quality of protein structures solved by NMR. J. Biomol. NMR. 1996;8:477–486.

[37] Colovos C, Yeates TO. Verification of protein structures: patterns of nonbonded atomic interactions. Protein Sci. 1993;2:1511–1519.

[38] Zhang Z, Li Y, Lin B, et al. Identification of cavities on protein surface using multiple computational approaches for drug binding site prediction. Bioinformatics. 2011;27:2083–2088.

[39] Roy A, Yang J, Zhang Y. COFACTOR: an accurate comparative algorithm for structure-based protein function annotation. Nucleic Acids Res. 2012;40:W471–W477.

[40] Yang J, Roy A, Zhang Y. Protein-ligand binding site recognition using complementary binding-specific substructure comparison and sequence profile alignment. Bioinformatics. 2013;29:2588–2595.

[41] Suzuki S, Nakanishi E, Ohira T, et al. Chitinase inhibitor allosamidin is a signal molecule for chitinase production in its producing Streptomyces I. Analysis of the chitinase whose production is promoted by allosamidin and growth accelerating activity of allosamidin. J. Antibiot. (Tokyo). 2006;59:402–409.

[42] Khan FI, Shahbaaz M, Bisetty K, et al. Large scale analysis of the mutational landscape in beta-glucuronidase: a major player of mucopolysaccharidosis type VII. Gene. 2016;576:36–44.

[43] Stephens DE, Khan FI, Singh P, et al. Creation of thermostable and alkaline stable xylanase variants by DNA shuffling. J. Biotechnol. 2014;187:139–146.

[44] Anwer K., Sonani R., Madamwar D., et al. Role of N-terminal residues on folding and stability of C-phycoerythrin: simulation and urea-induced denaturation studies. J. Biomol. Struct. Dyn. 2015;33:121–133.

[45] Khan FI, Aamir M, Wei DQ, et al. Molecular mechanism of Ras-related protein Rab-5A and effect of mutations in the catalytically active phosphate-binding loop. J. Biomol. Struct. Dyn. 2016:1–14.

[46] Van Der Spoel D., Lindahl E., Hess B., et al. GROMACS: fast, flexible, and free. J. Comput. Chem. 2005;26:1701–1718.

[47] Lopes P.E., Huang J., Shim J., et al. Force field for peptides and proteins based on the classical drude oscillator. J. Chem. Theor. Comput. 2013;9:5430–5449.

[48] Humphrey W., Dalke A., Schulten K.. VMD: visual molecular dynamics. J. Mol. Graph. 1996;14:27–38.

[49] Anwer K, Rahman S, Sonani RR, et al. Probing pH sensitivity of alphaC-phycoerythrin and its natural truncant: a comparative study. Int. J. Biol. Macromol. 2016;86:18–27.

[50] Still WC, Tempczyk A, Hawley RC, et al. Semianalytical treatment of solvation for molecular mechanics and dynamics. J. Am. Chem. Soc. 1990;112:6127–6129.

[51] Spassov VZ, Bashford D. Multiple-site ligand binding to flexible macromolecules: separation of global and local conformational change and an iterative mobile clustering approach. J. Comput. Chem. 1999;20:1091–1111.

[52] Spassov VZ, Yan L. A fast and accurate computational approach to protein ionization. Protein Sci. 2008;17:1955–1970.

[53] Flanagan MA, Ackers GK, Matthew JB. Electrostatic contributions to the energetics of dimer-tetramer assembly in human hemoglobin: pH dependence and effect of specifically bound chloride ions. Biochemistry. 1981;20:7439–7449.

[54] Song Y, Mao J, Gunner MR. MCCE2: improving protein pKa calculations with extensive side chain rotamer sampling. J. Comput. Chem. 2009;30:2231–2247.

[55] Matthew JB, Gurd FR, Garcia-Moreno B, et al. pH-Dependent processes in proteins. CRC Crit. Rev. Biochem. 1985;18:91–197.

[56] Yang AS, Honig B. On the pH dependence of protein stability. J. Mol. Biol. 1993;231:459–474.

[57] Machuqueiro M, Baptista AM.. The pH-dependent conformational states of kyotorphin: a constant-pH molecular dynamics study. Biophys. J. 2007;92:1836–1845.

[58] Wilkins MR, Gasteiger E, Bairoch A, et al. Protein identification and analysis tools in the ExPASy server. Methods Mol. Biol. 1999;112:531–552.

[59] Zhang Y. I-TASSER server for protein 3D structure prediction. BMC Bioinform. 2008;9:40. doi:http://dx.doi.org/10.1186/1471-2105-9-40.

[60] Kim DE, Chivian D, Baker D. Protein structure prediction and analysis using the Robetta server. Nucleic Acids Res. 2004;32:W526–W531.

[61] de Beer TA, Berka K, Thornton JM, et al. PDBsum additions. Nucleic Acids Res. 2014;42:D292–D296.

[62] Rao FV, Houston DR, Boot RG, et al. Crystal structures of allosamidin derivatives in complex with human macrophage chitinase. J. Biol. Chem. 2003;278:20110–20116.

[63] van Aalten DM, Komander D, Synstad B, et al. Structural insights into the catalytic mechanism of a family 18 exo-chitinase. Proc. Natl. Acad. Sci. U.S.A. 2001;98:8979–8984.

[64] Schuttelkopf A.W., Gros L., Blair D.E., et al. Acetazolamide-based fungal chitinase inhibitors. Bioorg. Med. Chem. 2010;18:8334–8340.

[65] Lobanov M, Bogatyreva NS, Galzitskaia OV. Radius of gyration is indicator of compactness of protein structure. Mol. Biol. (Mosk). 2008;42:701–706.

[66] Ivankov DN, Bogatyreva NS, Lobanov MY, et al. Coupling between properties of the protein shape and the rate of protein folding. PLoS ONE. 2009;4:e6476.

[67] Kuzmanic A, Zagrovic B. Determination of ensemble-average pairwise root mean-square deviation from experimental B-factors. Biophys. J. 2010;98:861–871.

[68] Maguid S, Fernandez-Alberti S, Echave J.. Evolutionary conservation of protein vibrational dynamics. Gene. 2008;422:7–13.

[69] Meng Zhang AKP, Govender A, Z Wang, et al. The multi-chitinolytic enzyme system of the compost-dwellingthermophilic fungus *Thermomyces lanuginosus*. Process Biochem. 2014.